A1 R HD25

High-Definition Resonant Scanning Confocal System

More Data, Faster

- Largest field of view on the market
- Acquire 2x the amount of data per scan
- Acquire larger fields of view without compromising resolution
- Long working distance optics for imaging organoids and organ-chips

Stunning High-Definition Images at Resonant Speed

- Acquire 1024 x 1024 high-definition images at high-speed
- AI-based noise removal from resonant scanned images

Powerful Acquisition and Analysis Tools

- Fully customizable acquisition and analysis workflows
- AI-enabled tools for image processing and analysis

www.microscope.healthcare.nikon.com/a1rhd25

Nikon Instruments Inc. • nikoninstruments.us@nikon.com • 1-800-52-NIKON

STEM CELLS®

TISSUE-SPECIFIC STEM CELLS

Peribiliary Glands as a Niche of Extrapancreatic Precursors Yielding Insulin-Producing Cells in Experimental and Human Diabetes

GUIDO CARPINO,[a] ROSA PUCA,[b] VINCENZO CARDINALE,[b] ANASTASIA RENZI,[c] GAIA SCAFETTA,[b] LORENZO NEVI,[b] MASSIMO ROSSI,[d] PASQUALE B. BERLOCO,[d] STEFANO GINANNI CORRADINI,[e] LOLA M. REID,[f] MARELLA MARODER,[b] EUGENIO GAUDIO,[c] DOMENICO ALVARO[b,g]

Key Words. Stem cell • Streptozotocin • Biliary tree • Endoderm • Regeneration • Peribiliary gland

ABSTRACT

Peribiliary glands (PBGs) are niches in the biliary tree and containing heterogeneous endodermal stem/progenitors cells that can differentiate, in vitro and in vivo, toward pancreatic islets. The aim of this study was to evaluate, in experimental and human diabetes, proliferation of cells in PBGs and differentiation of the biliary tree stem/progenitor cells (BTSCs) toward insulin-producing cells. Diabetes was generated in mice by intraperitoneal injection of a single dose of 200 mg/kg ($N = 12$) or 120 mg/kg ($N = 12$) of streptozotocin. Liver, pancreas, and extrahepatic biliary trees were en bloc dissected and examined. Cells in PBGs proliferated in experimental diabetes, and their proliferation was greatest in the PBGs of the hepatopancreatic ampulla, and inversely correlated with the pancreatic islet area. In rodents, the cell proliferation in PBGs was characterized by the expansion of Sox9-positive stem/progenitor cells that gave rise to insulin-producing cells. Insulin-producing cells were located mostly in PBGs in the portion of the biliary tree closest to the duodenum, and their appearance was associated with upregulation of *MafA* and *Gli1* gene expression. In patients with type 2 diabetes, PBGs at the level of the hepatopancreatic ampulla contained cells showing signs of proliferation and pancreatic fate commitment. In vitro, high glucose concentrations induced the differentiation of human BTSCs cultures toward pancreatic beta cell fates. The cells in PBGs respond to diabetes with proliferation and differentiation towards insulin-producing cells indicating that PBG niches may rescue pancreatic islet impairment in diabetes. These findings offer important implications for the pathophysiology and complications of this disease. STEM CELLS *2016;34:1332–1342*

SIGNIFICANCE STATEMENT

Peribiliary glands within biliary tree represent the niche of biliary tree stem/progenitors cells that are able to differentiate in pancreatic beta cells. Whether these cells play a role in insulin production in diabetes is unknown. Here, we demonstrated that in experimental and human diabetes, cells within peribiliary glands proliferate and commit toward insulin-producing cells. Peribiliary gland niche may rescue the pancreatic islet impairment in diabetes with important implications for the pathophysiology and complications of this disease.

INTRODUCTION

Peribiliary glands (PBGs) of human and murine biliary trees are niches containing heterogeneous stem/progenitor cells (biliary tree stem/progenitor cells, BTSCs) [1, 2]. BTSCs have been isolated from human (h) biliary trees, and their phenotype, self-renewal capability, and potentiality to differentiate into mature cells have been extensively characterized both in vitro and in vivo [3]. The hBTSCs express a broad panel of stem cell markers, have long-term (in vitro) persistence and self-renewal, and are able to lineage restrict to different mature cell fates [4]. The hBTSCs residing in PBGs are endowed with the capacity for pancreatic endocrine differentiation, and indeed they express biomarkers indicative of either an intermediate endocrine pancreas differentiation stage (Pdx1/Ngn3) or a mature islet cell stage, with some of the cells expressing insulin, depending on their location within the biliary tree [2, 5].

The embryological development of liver and pancreas in mammals is associated with the appearance of a common biliopancreatic progenitor, which differentiates in distinct lineages driven by specific transcriptional factors

[a]Department of Movement, Human and Health Sciences, University of Rome "Foro Italico,", Rome, Italy; [b]Department of Medico-Surgical Sciences and Biotechnologies; [c]Department of Anatomical, Histological, Forensic Medicine and Orthopedics Sciences; [d]Department of General Surgery and Organ Transplantation, and [e]Department of Clinical Medicine, Gastroenterology Division, Sapienza University of Rome, Rome, Italy; [f]Department of Cell and Molecular Physiology, Program in Molecular Biology and Biotechnology, University of North Carolina School of Medicine, Chapel Hill, North Carolina, USA; [g]Eleonora Lorillard Spencer-Cenci Foundation, Rome, Italy

Correspondence: Guido Carpino, M.D., Ph.D., Department of Movement, Human and Health Sciences, University of Rome "Foro Italico," Piazza Lauro De Bosis, 6 – 00135 Rome, Italy. Telephone: + 39-06-36733202; Fax:+39-06-36733202; e-mail: guido.carpino@uniroma1.it

Received July 27, 2015; accepted for publication December 2, 2015; first published online in STEM CELLS *EXPRESS* February 6, 2016.

1066-5099/2016/$30.00/0

http://dx.doi.org/10.1002/stem.2311

[6, 7]. Recently, Banga et al. [8] demonstrated that Sox9-positive cells in the biliary tree could be genetically reprogrammed to pancreatic cells with the appearance of ectopic duct-like structures in which cells express a variety of endocrine pancreatic markers in association with the improvement of a glycemic profile.

The aim of this study was to investigate whether PBGs and their associated hBTSCs could be involved in the pathophysiology of diabetes. In particular, in the streptozotocin (STZ)-induced experimental diabetes in murine (m) hosts, we evaluated the activation and proliferation of cells within PBGs and whether mBTSCs are capable of differentiating toward endocrine pancreatic islet fates. In humans, we evaluated the activation of the PBG compartment in the extrahepatic biliary tree (EHBT) of patients with type 2 diabetes (T2D) and the in vitro response of hBTSCs to high glucose concentrations.

Materials and Methods

Murine Model

Six-week-old male C57BL/6J mice ($N = 49$) were purchased from Charles River Laboratories (Wilmington, Massachusetts, MA, http://www.criver.com/) and housed at 22°C with 12:12 hour light/dark cycles. Animals were fasted overnight, and blood glucose levels were measured in an automatic glucose monitor (Accu-Check Compact Plus, Roche Diagnostics, Basel, Switzerland, CH, http://www.roche-applied-science.com) from the tail vein.

The following groups have been investigated:

- *High-dose STZ group*: Twelve mice were intraperitoneally injected with a single dose of 200 mg/kg of STZ (Sigma-Aldrich, St. Louis, Missouri, MO, http://www.sigmaaldrich.com) in 0.1 M citrate buffer pH 4.5 [9]. Nine mice were injected with the equivalent volume of citrate buffer as negative controls. Blood glucose levels were monitored at 1, 7, and 14 days after STZ treatment. We found that 12/12 (100%) of the mice were rendered diabetic (blood glucose levels $>$ 300 mg/dl) and were included in the study [10]. Diabetic and control mice were sacrificed after 14 days.
- *Low-dose STZ group*: Twenty mice were intraperitoneally injected with a single dose of 120 mg/kg of STZ. Eight mice were injected with the equivalent volume of citrate buffer as controls. Blood glucose levels were monitored at 1, 7, 30, 45, 60, 75, and 90 days after STZ treatment. We found that 12/20 (60%) mice were rendered diabetic (blood glucose levels $>$ 300 mg/dl) and were included in the study [10]. Diabetic mice were sacrificed after 30 days (low-dose STZ D30: $n = 6$) or after 90 days (low-dose STZ D90: $n = 6$) [8]. Control mice were sacrificed at 30 ($n = 4$) and 90 ($n = 4$) days after citrate buffer (the STZ carrier) injection.

At the end of the treatments, mice were sacrificed by cervical dislocation. Urine samples were obtained, drawn directly from the urinary bladder. Glucose concentration in the urine was measured by the Keto Diabur Test (Roche Diagnostics, Milan, Italy, https://www.accu-chek.it/it/prodotti/urinari/index.html?product=ketodiaburtest5000). The HbA1c concentration was measured by mouse glycated hemoglobin A1c (GHbA1c) ELISA Kit (cat # CSB-E08141M, DBA, Milan, Italy, http://www.arp1.com/Glycated-hemoglobin-A1c-GHbA1c-Mouse-ELISA-p/csb-e08141m.htm).

The study was approved by our local ethical committee at Sapienza University of Rome. All animal experiments were approved by the institutional animal care and use committee of Sapienza University of Rome. *Guide for the Care and Use of Laboratory Animals*, Eighth edition (2011) was followed.

Human Samples

hEHBT ($N = 10$) were obtained from cadaveric adult donors. All tissues derived from adult liver grafts from the surgical department of Sapienza University of Rome, Italy. Informed consent was obtained from next of kin for use of the tissues for research purposes, the study protocols received Institutional Review Board approval, and processing was compliant with Good Manufacturing Practice. On the basis of anamnestic and serological data, samples were divided into normal ($N = 5$) or T2D ($N = 5$).

Light Microscopy and Immunohistochemistry

The murine EHBT (mEHBT) was dissected en bloc [11] using a Surgical Microscope Zeiss (Zeiss OP-MI6 SD; Carl Zeiss, Goettingen, Germany, http://www.zeiss.com/microscopy/en_de/home.html) equipped with a digital videocam (Panasonic GP-KS162, Milan, Italy, http://www.panasonic.com/it/). The gallbladder was individuated and dissected; then, the dissection proceeded along cystic duct, common bile duct, and hepatopancreatic ampulla. Finally, the portion of duodenum near the hepatopancreatic ampulla was cut, and the entire mEHBT was collected (Fig. 1A).

The mEHBTs were fixed en bloc in 10% buffered formalin and embedded in paraffin (55°C–57°C); serial 3 μm-sections were obtained and stained with hematoxylin & eosin and Masson's trichrome. Three to five serial sections were examined for each specimen. At least three transversal-sectioned ducts were scanned by a digital scanner (Aperio Scanscope CS System, Aperio Technologies, Oxford, U.K., http://www.leicabiosystems.com/digital-pathology/aperio-digital-pathology-slide-scanners) and processed by ImageScope [12]. Transversal diameter was calculated for each duct (Fig. 1B, upper). No significant differences were present among all examined ducts. The mean of diameters of examined ducts was not significantly different among groups. Pancreatic tissue at the level of the spleen hilum and liver samples were also collected and processed.

Human pancreas, duodenum, and part of the EHBT were obtained en bloc from routine orthotopic liver transplantation procedures. The duodenal wall was sectioned, and the major papilla was individuated. The head of the pancreas was dissected, and the main pancreatic duct, the common bile duct (choledocus), and the hepatopancreatic common duct were visualized. For each case, human samples were taken at the level of the hepatopancreatic ampulla. Human samples were fixed in 10% buffered formalin and embedded in paraffin (55°C–57°C) and processed for routine histological stains.

The PBG area was calculated as the volume fraction occupied by PBG/total duct area and expressed as a percentage both in mice (Fig. 1A, lower) and in human samples [13]. The pancreatic islet area was measured by an image analysis system (IAS—Delta Sistemi, http://www.delta-sistemi.it, Rome, Italy) as the volume fraction occupied by islet/pancreatic area and expressed as a percentage.

For immunohistochemistry, sections were incubated overnight at 4°C with a primary antibody against proliferating cellular nuclear antigen (PCNA: mouse monoclonal; code: M0879; dilution: 1:50; Dako, Glostrup, Denmark, http://www.

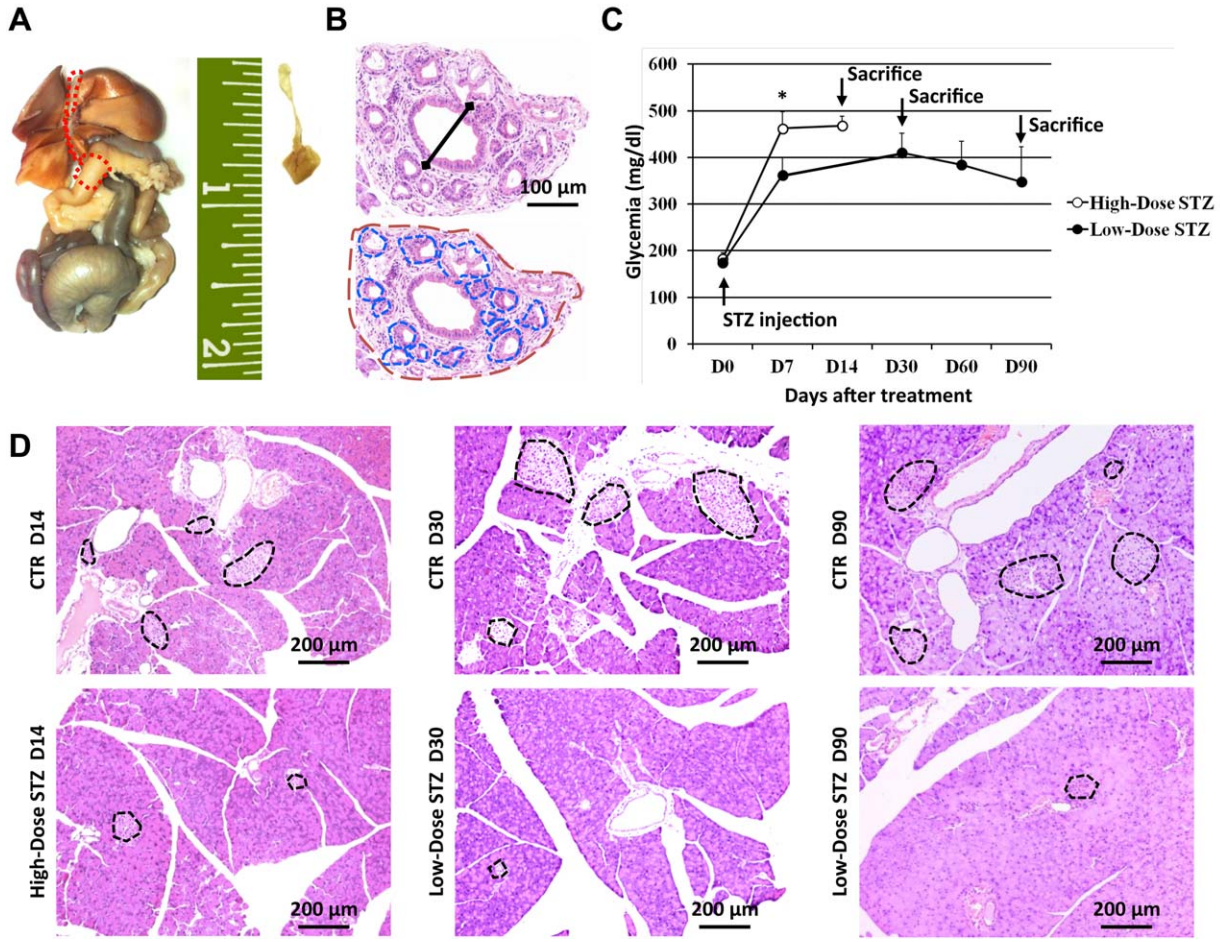

Figure 1. Models of experimental induced diabetes. **(A)**: Isolation and surgical removal of the mouse extrahepatic biliary tree (EHBT). **(B)**: Hematoxylin and eosin (H&E) stains. EHBT (line in upper image) has been assessed in transversal section of the duct. Peribiliary gland area has been calculated as the percentage of area occupied by glandular acini (blue line) with respect to the duct total area (red line). Original magnification: × 20. **(C)**: Blood glucose levels in high-dose STZ-treated mice and low-dose STZ-treated mice. *, $p < .01$ versus low-dose STZ-treated mice. **(D)**: H&E staining of pancreas in control and STZ-treated mice. In STZ-treated mice there was a reduction of pancreatic islet area (circles) in comparison with controls. Original magnification: × 10. Abbreviations: CTR, control; D, day; STZ, Streptozotocin.

dako.com) and Neurogenin 3 (Ngn3: rabbit polyclonal; code: AB5684; dilution: 1:100; Millipore, Milan, Italy, http://www.millipore.com). Samples were rinsed twice with phosphate buffered saline (PBS) for 5 minutes, incubated for 20 minutes at room temperature (RT) with secondary biotinylated antibody, and then with Streptavidin-horseradish peroxidase (HRP) (LSAB + System-HRP, Dako, code K0690). Diaminobenzidine (Dako) was used as substrate, and sections were counterstained with hematoxylin [14].

For immunofluorescence, nonspecific protein binding was blocked by 5% normal goat serum. Specimens were incubated with primary antibodies against Sox9 (rabbit polyclonal; code: AB5809; dilution: 1:50; Millipore, Billerica, MA) and Insulin (Dako, guinea pig polyclonal; code: IS002 dilution: 1:50). Then, specimens were incubated for 1 hour at RT with labeled isotype-specific secondary antibodies (Alexafluor, Invitrogen, Life Technologies, Paisley, U.K., http://www.invitrogen.com) and counterstained with 4′,6-diamidino-2-phenylindole (DAPI) for visualization of cell nuclei. For all immunoreactions, negative controls were also included.

Sections were examined by Leica Microsystems DM 4500 B Microscope (Weltzlar, Germany) equipped with a Jenoptik Prog Res C10 Plus Videocam (Jena, Germany). Immunohistochemistry/immunofluorescence observations were processed with an IAS—Delta Sistem and were independently performed by two researchers in double blind fashion [15]. For quantitative analysis, slides were scanned by a digital scanner (Aperio CS2 for bright field and Aperio FL for immunofluorescence, Aperio Technologies, Oxford, U.K.) and processed by ImageScope. An image analysis algorithm was used to quantify the percentage of cells with PCNA, Sox9, and Ngn3 nuclear expression within PBGs. The number of positive cells has been calculated as the percentage of cells with positive nuclei with respect to the total number of cells within PBGs. Similarly, an image analysis algorithm has been used to quantify the percentage of insulin-positive cells within PBGs. The number of positive cells has been calculated as the percentage of positive cells with respect to the total number of cells within PBGs. Counts have been performed in all glandular acini in each examined ducts.

Reverse-Transcription Polymerase Chain Reaction Analysis

Total RNA was extracted by the procedures of Chomczynski and Sacchi [16]. RNA quality and quantity was evaluated with the Experion Automated Electrophoresis System. RNA

equipped with the RNA StSens Analysis Chip (Bio-Rad Laboratories, Hercules, CA, http://www.bio-rad.com) was done as previously described [17]. RNA was extracted by TRIZOL reagent (Life Technologies, Rockville, MD, http://www.lifetech.com; Cat# 15596-026) according to the manufacturer's instructions. 1 μg of RNA was retrotranscribed using High Capacity cDNA Reverse Transcription Kit (Applied Biosystems, Life Technologies, Paisley, U.K., http://www.appliedbiosystems.com: cod. 4368814), and cDNA was amplified using SensiMix SYBR kit (Bioline, London, U.K.: cod. QT605-05, http://www.bioline.com/us/sensimix-sybr-hi-rox-kit.html) according to the manufacturer's instructions.

The primers used were: *Gli1*: fw ACAAGTGCACGTTTGAA GGCTGTC, rev GCTGCAACCTTCTTGCTC; *Insulin*: fw TATAAA GCTGGTGGGCATCC, rev GCCATGTTGAAACAATGAC; *Mafa*: fw TTCTCCTTGTACAGGTCCCG, rev GAGAGCGAGAAGTGCCAACT; *Ngn3*: fw CTTCGTCTTCCGAGGCTCT rev CTATTCTTTTGCGCCGGTA G; *18s*: fwGCAATTATTCCCCATGAACG, rev GGGACTTAATCAA CGCAAGC.

The expression of the gene of interest was calculated by the ratio of the concentrations of the gene of interest and the reference gene *18s*.

Protein Extraction from Paraffin Embedded Samples and ELISA for Insulin

Total proteins were extracted from formalin fixed paraffin embedded (FFPE) sample block using the Qproteome FFPE Tissue Kit (Qiagen, catalog # 37623, Qiagen Srl, Milan, Italy, http://www1.qiagen.com). Briefly, three serial, 15 μm thick sections were obtained from the same FFPE block for each sample. Sections were immediately placed in a 1.5 ml collection tube; then, deparaffinization and protein extraction was performed as indicated by the vendor. The tissue content of mouse insulin was measured by Mouse Ultrasensitive Insulin ELISA (ALPCO, catalog # 80-INSMSU-E01, E10; Salem, US, http://w.alpco.com/products/Insulin_Ultrasensitive_Mouse_ELISA.aspx), normalized to the volume of the origin tissue sample, and expressed as ng/ml per mm^3 of tissue.

Human BTSC Isolation and In Vitro Studies

hBTSCs were obtained from organ donors from the ''Paride Stefanini'' Department of General Surgery and Organ Transplantation, Sapienza University of Rome, Rome, Italy. Informed consent was obtained. Tissue specimens were processed as described previously [3]. Cells were sorted for EpCAM (Miltenyi Biotec S.r.l., Bologna, Italy, http://www.miltenyibiotec.com) by using magnetic beads [5]. Isolated hBTSCs were seeded onto culture plastic at a density of 9×10^4 cells per cm^2 or 2.5×10^4 cells per cm^2 and cultured in serum-free Kubota's Medium (KM), a medium permissive for self-replication of endodermal stem cells. Two culture conditions were tested:

- *Basal* (glucose concentration: 11 mM): KM (pH 7.4) was used.
- *High glucose concentrations* (glucose concentration: 22 mM): (+)-D-glucose (Sigma-Aldrich, St. Louis, Missouri, MO) was added in KM to a final concentration of 22 mM (pH 7.4).

Total RNA was extracted at 7 days and 14 days, and reverse transcription polymerase chain reaction (RT-PCR) analysis was performed. Immunofluorescence analysis was performed at 14 days.

Measurement of C-Peptide Secretion in hBTSCs

The hBTSCs were plated at 100,000 cells per well in 12-well plates (3.85 cm^2 surface area per well) and cultured in KM at basal (11 mM) or high glucose (22 mM) concentration for 14 days. Medium was replaced every day. After 14 days, the medium was removed, and the cultures washed twice with PBS without calcium and magnesium. Medium was added to the cells, incubated for 24 hours from each well of a 12-well plate seeded with 100,000 cells per well, and then was collected and stored at −20°C. After media collection, the cells were collected separately from each well and counted using the Trypan blue exclusion assay. The human C-peptide concentration in the medium of each well was measured by an ELISA kit (Mercodia cod. N. 10-1136-01; Uppsala, Sweden, https://www.mercodia.com/index.php?page=productview2&prodId=13), normalized to the cell number of each sample, and expressed as levels per 100,000 cells. Normal pancreatic islet cells were purchased by ProdoLab, Irvine CA (HIR-001, http://prodolabs.com) and used as positive controls. HepG2 cells were purchased commercially from ATCC (No. HB-8065, Georgetown University in Washington, DC, US; http://www.atcc.org/products/all/HB-8065.aspx) and were used as a negative control.

Statistical Methods

Continuous normally distributed variables are summarized and presented as mean ± SEM. To compare the means between groups for normally distributed data, analysis of variance or the Student's *t* test was performed. To determine differences between groups having not normally distributed data, medians were tested by Mann–Whitney *U* tests. The Pearson correlation coefficient was used to determine correlations between continuous normally distributed variables. The degree of association between nonparametric or ordinal variables was assessed using the Spearman nonparametric correlation. Statistical significance was set to a p value $< .05$. Statistical analysis was performed by SPSS statistical software (SPSS, Chicago, IL)

Results

STZ-Induced Experimental Diabetes: Biochemical Parameters

STZ resulted in an increase of glycemia (Fig. 1; Supporting Information Tables 1, 2), glucose urinary levels (not shown), and HbA1c (not shown) in comparison with controls.

In the high-dose STZ group, 12/12 mice showed a rapid and marked increase of glycemia at 7 days, and this was sustained until beyond 14 days, when the mice were sacrificed (Fig. 1C; Supporting Information Table 1). High-dose STZ-treated mice showed high urinary glucose levels at death, and HbA1c was significantly increased (not shown).

In the low-dose STZ group, mice showed a less rapid increase of glycemia in comparison with mice treated with high dose of STZ. At D7, low-dose STZ group presented lower glycemic levels in comparison with high-dose STZ group ($p < .05$; Fig. 1C). Consistently, only 12/20 mice treated with lower doses of STZ became diabetic. As shown in Figure 1C and Supporting Information Table 2, in the low-dose STZ group, glycemia reached the highest levels at D30 and then stabilized.

Table 1. Morphometric and immunohistochemical analysis

	Control	High-dose STZ D14	Low-dose STZ D30	Low-dose STZ D90
Pancreatic islet area (μm^2)	1.93 ± 0.94	0.55 ± 0.52*	0.21 ± 0.11*	0.31 ± 0.27*
Bile duct diameter (μm)	117 ± 18.4	123.3 ± 13.7	119.9 ± 22.8	124.2 ± 31.2
PBG area (μm^2)	5.05 ± 1.98	7.17 ± 1.72*	8.73 ± 2.09*	11.63 ± 3.64**
PAS-positive PBG cells (%)	3.3 ± 1.5	18.3 ± 3.5*	44.5 ± 4.0*,***	39.0 ± 4.6*
PCNA-positive PBG cells (%)	7.2 ± 1.9	35.8 ± 4.7*	37.4 ± 3.4*	23.6 ± 5.4**
Sox9-positive PBG cells (%)	16.2 ± 4.6	59.0 ± 4.5*	57.4 ± 7.7*	36.8 ± 7.5**
Ngn3-positive PBG cells (%)	17.1 ± 1.3	53.1 ± 5.6*	48.0 ± 8.7*	25.2 ± 4.9**
Insulin-positive PBG cells (%)	Negative	6.0 ± 3.1*	7.0 ± 3.1*	41.6 ± 15.7**

D, day; PAS, Periodic Acid Schiff; PBG, peribiliary gland; STZ, streptozotocin.
* $p < .05$ versus control group.
** $p < .05$ versus other groups.
*** $p < .05$ versus high-dose STZ D14 group.

In STZ-treated mice, glucose serum levels correlated with glucose urinary levels ($r = .942$, $p < .001$) and HbA1c ($r = .817$, $p < .001$) while no differences were found among the three (mice sacrificed at 14, 30, or 60 days after citrate buffer injection) control groups.

Pancreatic Islet Area and PBG Area in Normal and STZ Mice

Treatment with STZ resulted in a reduction of pancreatic islet area (Table 1). These values were significantly decreased compared with that in normal pancreas ($p < .05$ vs. STZ groups) (Fig. 1D). Insulin expression in pancreatic tissue in STZ-treated mice was reduced in comparison with controls (not shown). Interestingly, the level of pancreatic islet area was inversely correlated with glycemia ($r = -.691$, $p < .001$), HbA1c ($r = -.558$, $p < .01$), and glucose urinary levels ($r = -.652$, $p < .02$). No difference between the three control groups in term of pancreatic islet area was observed (not shown).

We next evaluated the extension of the PBG area within EHBTs (Fig. 2). No differences in PBG area were found among the three control groups (not shown), and this was consistent with similar glycemic profiles and pancreatic islet area. Accordingly, all control mice were analyzed as a single group ($n = 17$). The PBG area (Table 1) was significantly expanded in the high-dose STZ group and in the low-dose STZ group in

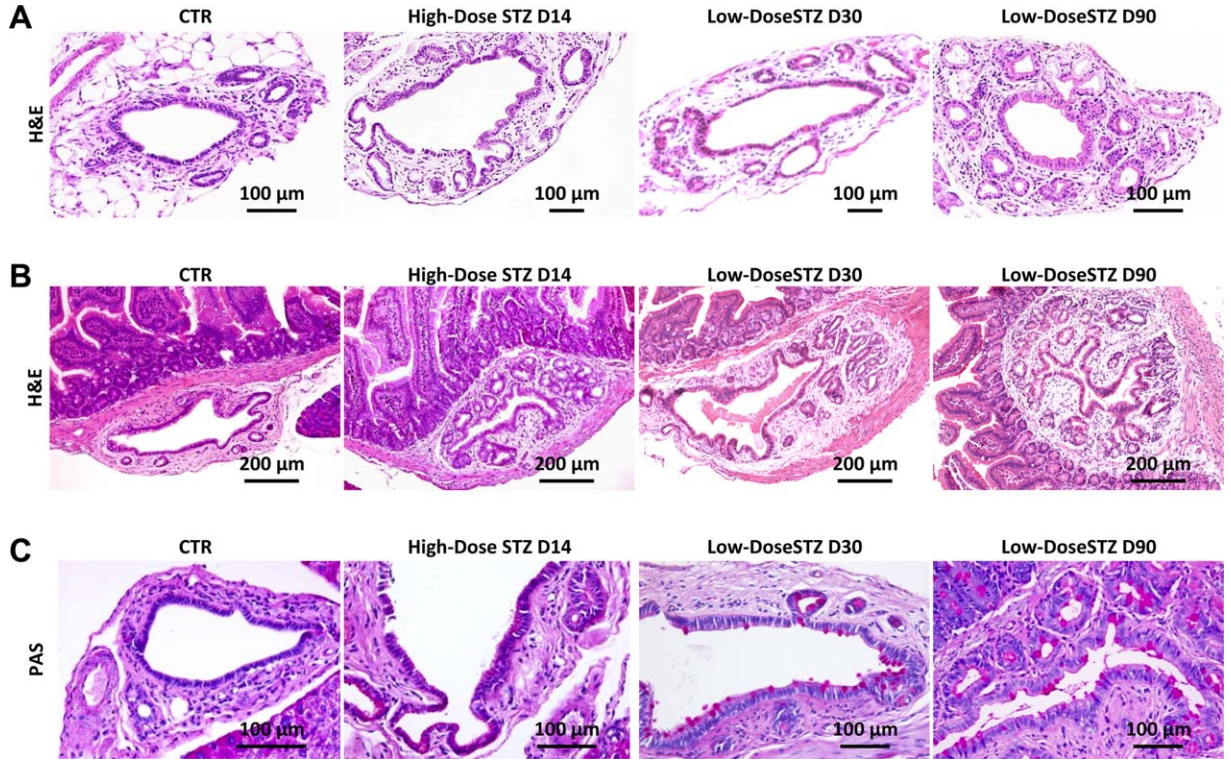

Figure 2. Peribiliary glands (PBGs) in induced experimental diabetes. **(A)**: Hematoxylin and eosin (H&E) staining of extrahepatic biliary tree (EHBT) in control and STZ-treated samples. At the level of the EHBT, STZ-treated mice showed a significant expansion of the PBG area after high-dose STZ treatment and after 30 days (D30) and 90 days (D90) of low-dose STZ treatment in comparison with controls. Original magnification: × 20. **(B)**: H&E staining of hepatopancreatic ampulla in control and STZ-treated samples. At the level of the hepatopancreatic ampulla, STZ-treated mice showed a significant expansion of PBG area after high-dose STZ treatment, and after 30 and 90 days of low-dose STZ treatment in comparison with controls. Original magnification: × 20. **(C)**: PAS staining of EHBT in control and STZ-treated samples. STZ treatment resulted in an increase of PAS-positive cells within PBGs. Original magnification: × 20. Abbreviations: CTR, control; PAS, Periodic Acid Schiff; STZ, streptozotocin.

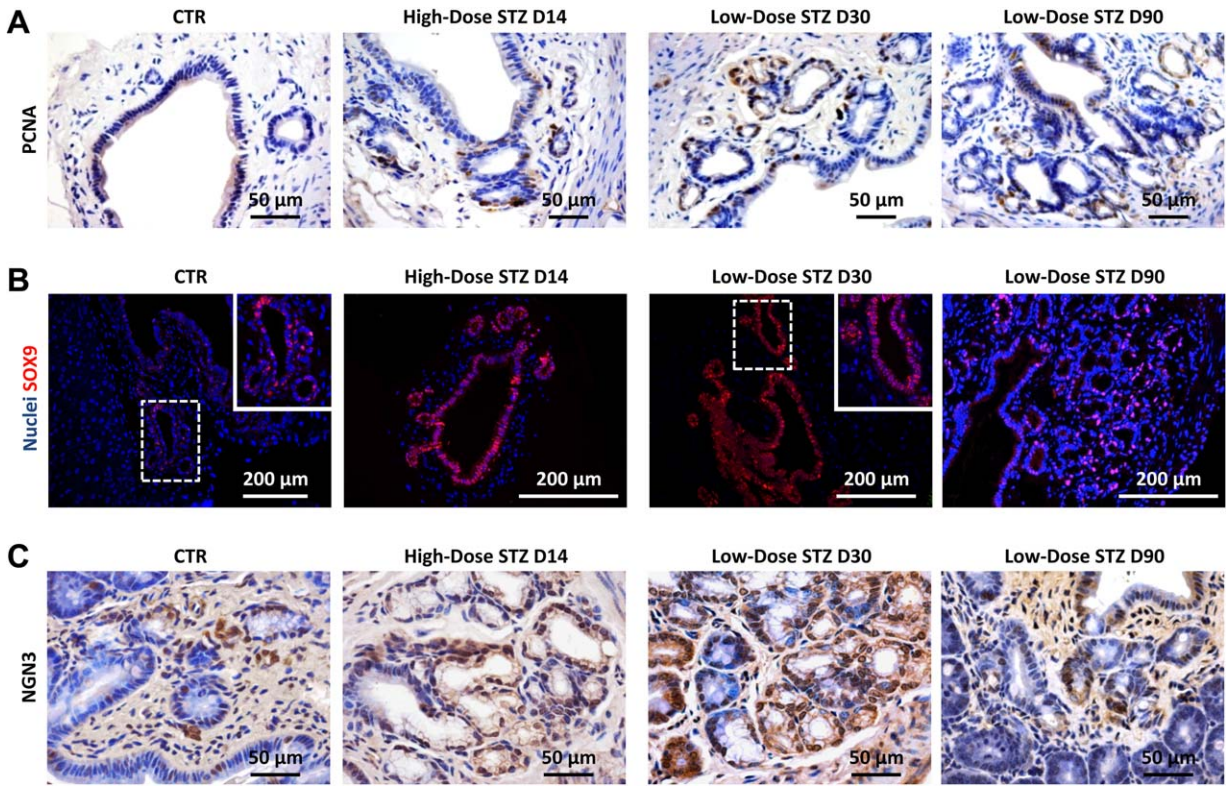

Figure 3. Activation of progenitor cell compartment in peribiliary glands (PBGs). **(A)**: Immunohistochemistry for PCNA. The number of PCNA-positive cells in PBGs increased after STZ treatment when compared to controls. Original magnification: × 40. **(B)**: Immunofluorescence for Sox9 (red) in extrahepatic biliary tree (EHBT) in control and STZ-treated mice. The percentage of Sox9-positive cells increased in STZ-treated mice in comparison with control (CTR) mice. Original magnification: × 20. **(C)**: Immunohistochemistry for Ngn3 in EHBT in control and (STZ)-treated mice. The percentage of Ngn3-positive cells increased in STZ-treated in comparison with control (CTR) mice. Original magnification: × 40. Abbreviations: CTR, control; NGN3, Neurogenin 3; PCNA, proliferating cell nuclear antigen; STZ, streptozotocin.

comparison with control mice ($p < .02$). In the low-dose STZ group, the PBG area was significantly higher at D90 compared to mice sacrificed at D30 ($p < .05$) or to high-dose STZ treated mice ($p < .05$). All examined ducts were comparable in size (Table 1). Interestingly, the PBG area was inversely correlated with those of pancreatic islets ($r = -.664$, $p < .05$). The increase of PBGs was also evident at the level of hepatopancreatic ampulla where the highest levels of PBG area were evident (23.35 ± 4.58 in the low-dose STZ D90 versus 10.87 ± 2.83 in controls; $p < .01$; Fig. 2B).

We next analyzed the phenotypic traits of cells in PBGs. STZ treatment dictated an increase of Periodic Acid Schiff-positive cells within PBGs when compared to controls (Fig. 2C). In accordance with PBG expansion, the number of proliferating (PCNA-positive) cells within PBGs was increased after STZ treatment when compared to controls (Fig. 3A).

The increase of PBG area in STZ-treated mice was characterized by the expansion of Sox9-positive stem/progenitor-like cells (Fig. 3B; Table 1). In normal PBGs, Sox9-positive cells represented a small population, restricted to deeper PBG acini. In high-dose D14 and low-dose D30 STZ-treated mice, Sox9-positive cells sprouted toward the surface and represented most of the PBG cells and surface epithelial cells ($p < .05$). When low-dose STZ mice were examined after 90 days of treatment, a lower percentage of Sox9-positive cells was present in comparison with other STZ treated groups ($p < .05$).

STZ-treated mice were also characterized by the expansion of Ngn3-positive stem/progenitor-like cells (Fig. 3C; Table 1) within PBGs. In high-dose D14 and low-dose D30 STZ-treated mice, Ngn3-positive cells sprouted toward the surface and represented most of the PBG cells and surface epithelial cells ($p < .05$ versus normal mice). Interestingly, when low-dose STZ mice were examined after 90 days of treatment, a lower percentage of Ngn3-positive cells was present in comparison with other STZ treated groups ($p < .05$).

PBG Cells Expressed Insulin After STZ Treatment

In normal mice, insulin was expressed in beta cells within pancreatic islets; whereas, acinar cells, pancreatic ducts, EHBT and associated PBGs were essentially insulin-negative (Fig. 4A; Table 1). In the high-dose STZ group, few cells within PBGs were insulin-positive. Similarly, in the low-dose STZ group, at D30, few cells within PBGs showed positivity for insulin. Interestingly, this percentage massively and significantly increased in mice sacrificed after 90 days ($p < .05$ vs. low-dose STZ, D30, and high-dose STZ, D14, groups); in the low-dose STZ group at D90, also surface epithelial cells were diffusely positive for insulin (Fig. 4A).

We next investigated in the low-dose STZ D90 group, the distribution of insulin-expressing cells along the EHBT. Interestingly, a gradient of insulin expression was evident with a lower number of positive cells in PBGs of the cystic duct and

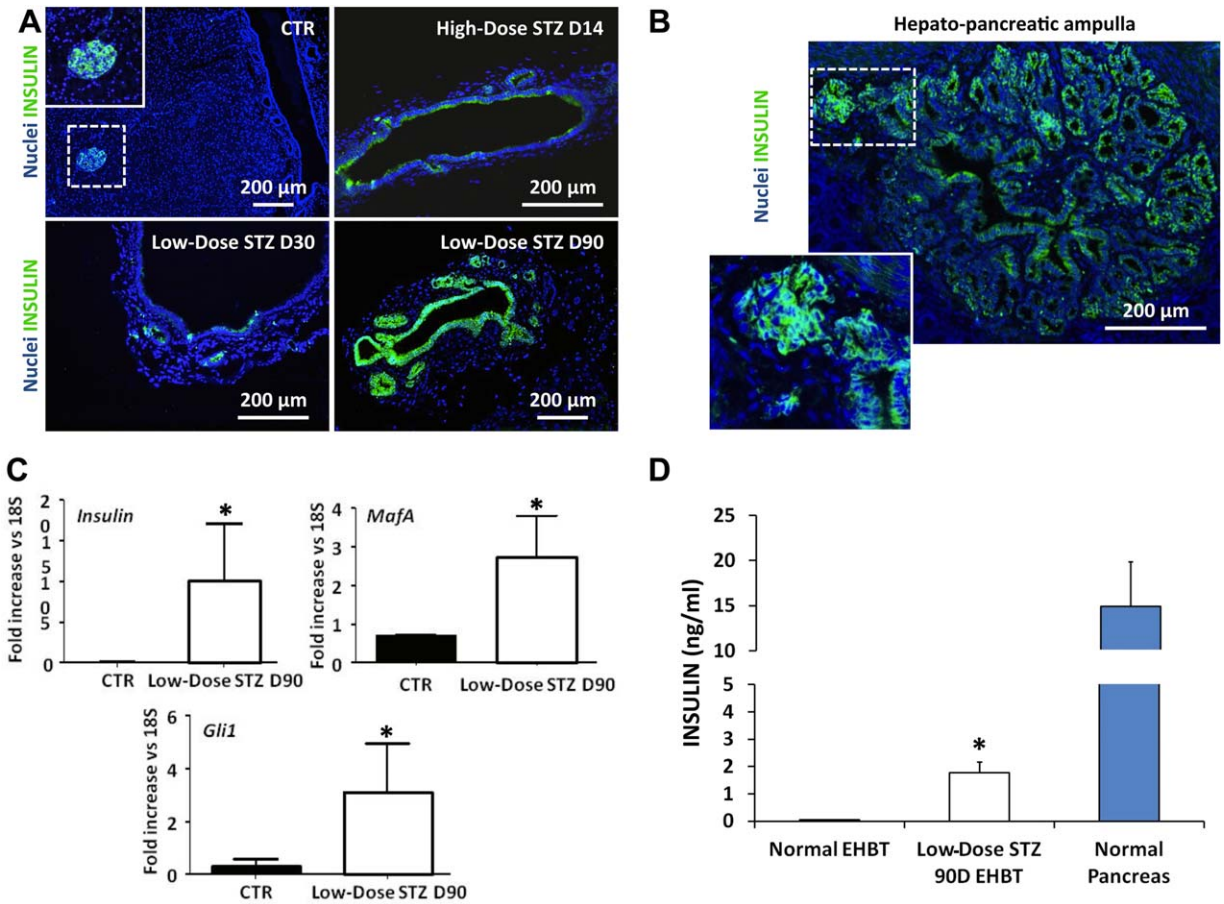

Figure 4. Differentiation of stem/progenitor cells of peribiliary glands (PBG) toward insulin-producing cells. **(A)**: Immunofluorescence for Insulin (green) in pancreas and EHBT in control and STZ-treated samples. In STZ-treated mice, peribiliary gland (PBG) cells were positive for insulin; positive cells mostly increased in number after 90 days (D90) of low-dose STZ treatment. Original magnification: × 20. **(B)**: In the hepatopancreatic ampulla after 90 days of low-dose STZ treatment, insulin was diffusely expressed in PBG cells and in the surface epithelium; islet-like structures could be found occasionally at the bottom of glandular elements (magnified at × 40). Original magnification: × 20. **(C)**: EHBT tissue showed a significant increase in *Insulin, MafA*, and *Gli1* gene expression in low-dose STZ after 90 days of treatment in comparison with controls.*, $p < .05$ versus CTR. **(D)**: ELISA tests for insulin: EHBT tissue samples showed a significant increase in insulin content in low-dose STZ after 90 days of treatment in comparison with normal EHBT samples.*, $p < .05$ versus other groups. Abbreviation: STZ, streptozotocin.

hilar hepatic duct and a higher number in the distal choledocus and hepatopancreatic ampulla. In particular, at the level of the hepatopancreatic ampulla, insulin was diffusely expressed in PBG cells and surface epithelium, and islet-like structures could occasionally be found at the bottom of glandular elements (Fig. 4B). In the low-dose STZ D90, but not in the other groups, insulin expression within PBG cells was inversely correlated with glycemic levels ($r = -.66$; $p < .05$).

Immunohistochemical data on biliary tree samples were confirmed by RT-PCR. RT-PCR was performed in specimens taken at the level of the liver hilum. These specimens were divided into two parts that were separately processed for RT-PCR and histology. Histological examination ruled out the presence of pancreatic tissue within liver specimens. Immunohistochemistry demonstrated that hepatocytes and interlobular bile ducts were constantly negative for insulin in all groups (not shown). By RT-PCR, EHBT tissues showed a significant increase in *insulin*, *MafA* and *Gli1* gene expression in the low-dose STZ D90 versus controls (Fig. 3D; $p < .05$). In contrast, *Insulin, MafA*, and *Gli1* gene expression levels were similar between low-dose STZ D30, high-dose STZ D14, and controls (data not shown).

Finally, to confirm insulin production at protein levels, ELISA tests for insulin were performed on tissue extracts (Fig. 4D). Insulin content increased in EHBT tissue in the low-dose STZ D90 group in comparison with normal ($p < .05$); insulin content in EHBT tissue from the low-dose STZ D90 group was decreased with respect to the normal pancreatic tissue ($p < .01$).

Proliferation of Human PBG Cells and Insulin Expression Were Increased in Hepatopancreatic Ducts from T2D Patients

In adult human T2D samples, the PBG area (Fig. 5A) at the level of hepatopancreatic ampulla was significantly expanded ($30{,}350\ \mu m^2 \pm 1{,}922$; $7.58\% \pm 0.68$) in comparison with normal subjects ($23{,}890\ \mu m^2 \pm 1{,}806$; $5.68\% \pm 0.55$; $p < .01$). In keeping with PBG expansion, the number of proliferating (PCNA-positive, Fig. 5A) cells within PBGs was increased in T2D ($55\% \pm 5$) when compared to normals ($36.7\% \pm 5.6$, $p < .01$; Fig. 5A). Consistently, in the T2D samples (at the

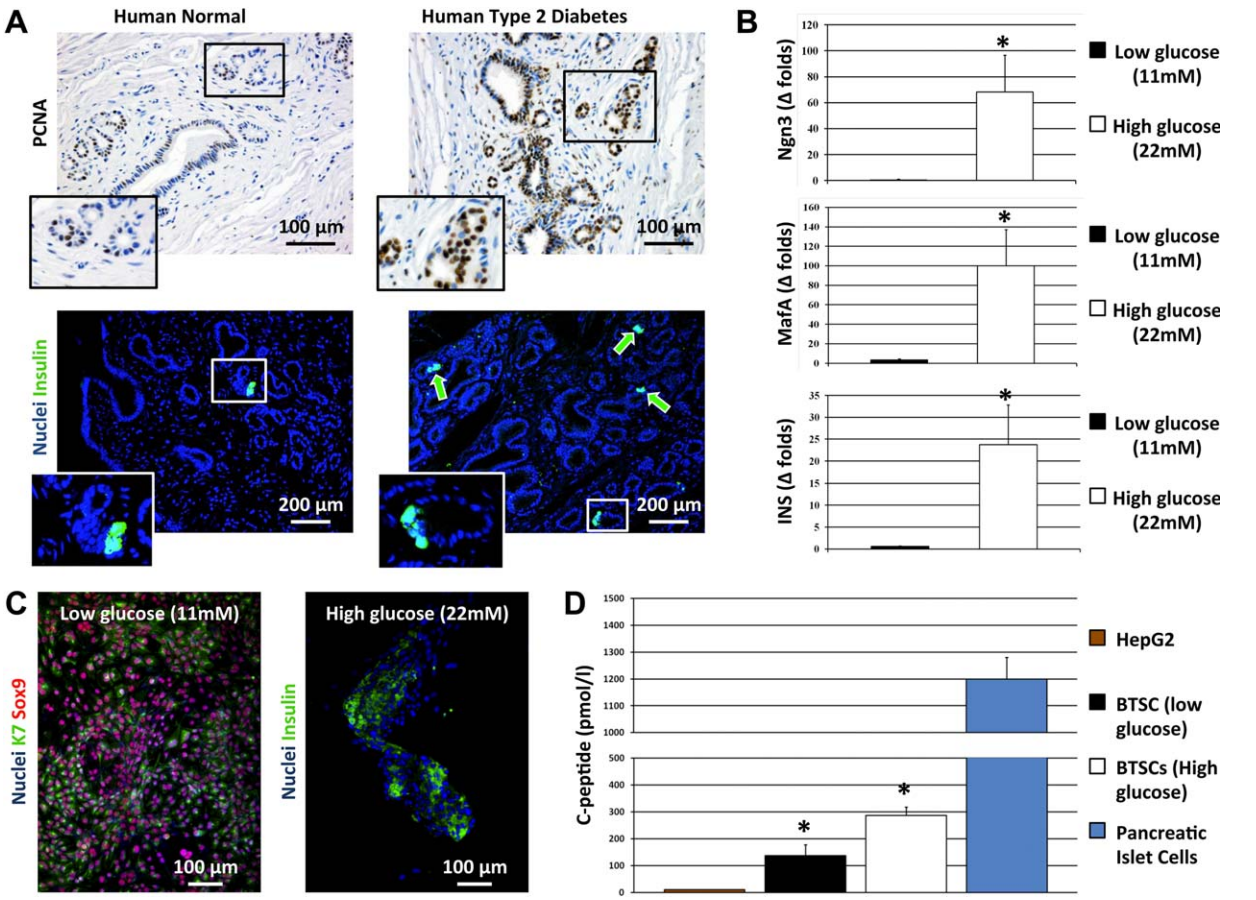

Figure 5. Human BTSC in type 2 diabetic patients and their in vitro response to high glucose. **(A)**: Immunohistochemistry for PCNA (upper) and immunofluorescence for insulin (lower). Peribiliary gland (PBG) area and the number of PCNA (proliferating cells) and insulin positive cells within PBGs were increased in biliary tree specimens obtained from type 2 diabetic patients in comparison with normal controls. Original magnification (OM): × 20 (upper) and ×10 (lower). Area in the boxes is magnified in the inserts. **(B–D)**: Human BTSCs isolated from normal biliary trees were cultured in basal (low glucose concentration: 11 mM) conditions or exposed to high glucose concentration (22 mM). (B): After 14 days in high glucose concentration, the expression of *Ngn3, MafA*, and *Insulin* genes was significantly increased. *, $p < .01$. (C): Immunofluorescence for EpCAM, Sox9, and insulin. In basal conditions, cultures were mostly composed of EpCAM-positive and Sox9-positive cells. After 14 days in high glucose concentration, insulin-positive cells appeared. Original magnification: × 20. KM: Kubota's medium, a serum-free medium designed for endodermal stem/progenitors. (D): ELISA test for C-peptide further confirmed the increasing of insulin production by human BTSCs at protein level and its secretion in the culture medium after incubation in high glucose concentration in comparison with basal conditions (*, $p < .05$ vs. others). Pancreatic islet and HepG2 cells were used as positive and negative controls, respectively. Abbreviations: BTSC, biliary tree stem/progenitor cell; Ngn3, Neurogenin 3; PCNA, proliferating cell nuclear antigen.

hepatopancreatic ampulla), a higher percentage of cells within PBGs were insulin positive (13.67% ± 5.13) in comparison with normals (6% ± 1; $p < .05$).

In Vitro Effects of High Glucose Concentrations on hBTSCs

BTSCs were isolated from human EHBT. The (+)-D-glucose concentration was doubled in the media of human BTSCs and, after 7 and 14 days, RT-PCR analyses were carried out. As shown in Figure 5B, after 14 days, the gene expression for *Ngn3, MafA*, and *Insulin* was markedly increased ($p < .01$; $n = 5$). By immunofluorescence, in basal conditions almost all cells were positive for stem cell markers (EpCAM and Sox9) and negative for insulin (not shown); after 14 days in high glucose concentration, the appearance of islet-like structures composed of densely packed insulin-positive cells was observed (Fig. 5C). In addition, ELISA tests for C-peptide further confirmed insulin production at the protein level, and its secretion in the culture medium after incubation in high glucose concentration in comparison with basal conditions ($p < .05$ vs. basal conditions; Fig. 5D).

Discussion

The PBGs in mice and in humans have been shown to contain stem/progenitors that respond to regenerative demands imposed by diabetes. The main findings of our study (Fig. 6) indicate that: (a) cells within PBGs proliferated in an experimental model of type 1 diabetes. The proliferation was greatest at the hepatopancreatic ampulla following decreased pancreatic islet area; (b) proliferation of cells within PBGs was associated with the expansion of the Sox9-positive stem/progenitor cell compartment. In bile ducts of normal mice, the BTSC compartment resided at the bottom of PBGs, while in diabetic mice it expanded occupying most of the glandular elements and the surface epithelium; (c) Sox9-positive BTSCs within PBGs became insulin-producing cells in diabetic mice in which they were

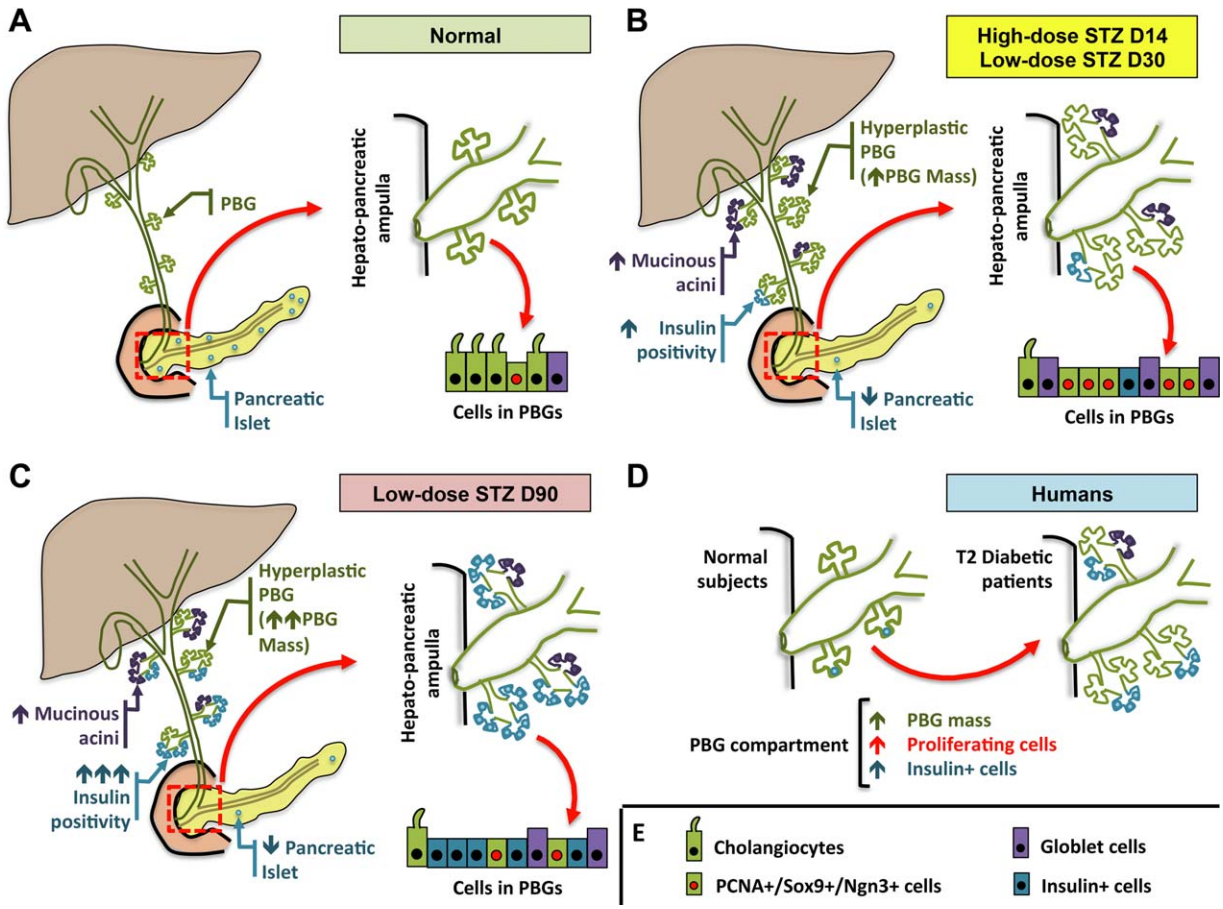

Figure 6. Summary of key findings. **(A)**: PBG compartments are located throughout the extrahepatic biliary tree but not in the gallbladder. PBGs are more numerous at the level of the hepatopancreatic ampulla. They are composed of cholangiocytes, goblet cells, and Sox9 + BTSC. **(B)**: In our experimental models, the administration of high and low doses of STZ determined the reduction of pancreatic islets and a correlated increase of PBG mass. PBGs are characterized by the expansion of proliferating Sox9+/Ngn3 + BTSCs, an increase in mucin production, and the appearance of insulin-producing cells within PBGs at 14 (D14) and 30 (D30) days after high- and low-dose STZ treatment, respectively. **(C)**: At 90 days (D90) after the administration of low-dose STZ, the number of insulin-producing cells within PBGs is highly increased; the greatest increase of PBG mass and insulin-producing cells occurs in the hepatopancreatic ampulla; **(D)** in humans, PBG hyperplasia, proliferation, and signs of endocrine pancreatic commitment are observable in hepatopancreatic ampulla specimens from type 2 (T2) diabetic patients in comparison with normal subjects. **(E)**: Legend of the cell type. Abbreviations: Ngn3, neurogenin 3; PBGs, peribiliary glands; PCNA, proliferating cell nuclear antigen; STZ, streptozotocin.

located mostly in the EHBT portion closest to the duodenum and displayed upregulation of *MafA* and *Gli1* gene expression. (d) In humans, PBG hyperplasia, proliferation, and signs of endocrine pancreatic commitment are observable in hepatopancreatic ampulla specimens from T2D patients. (e) With in vitro studies, hBTSCs responded to high glucose concentration with the upregulation of genes related to pancreatic islet cell commitment and the synthesis and secretion of c-peptide.

The human biliary tree has been shown to be a reservoir of stem and progenitor cells [1, 3–5, 18–20]. hBTSCs have been shown able to self-replicate under defined, serum-free conditions and then to be able to differentiate into either hepatocytes, cholangiocytes, or pancreatic islets dictated by the specifics of the differentiation conditions used [21]. When transplanted into immunocompromised mice, hBTSCs were able to repopulate cirrhotic liver and to correct experimentally induced diabetes depending on where the cells were transplanted [1, 3–5, 18–20].

Here, we investigated the behavior of the BTSC niche in experimental and human diabetes. In mice, diabetes was established at two different STZ dosages. The high-dose STZ model is characterized by a rapid increase of glycemic levels and high mortality [9], allowing only a short time for observation. The low-dose STZ model showed a slower increase of glycemia and longer survival, allowing a prolonged observation time [8, 10]. In both models, hyperglycemia was correlated with HbA1c, glucose urinary levels, and with pancreatic islet loss.

In STZ mice, a proliferation of cells within PBGs was evident. In the high-dose STZ model, PBG area rapidly increased within 14 days; in the low-dose STZ model, PBG area increased significantly after 30 days, and cells within PBGs continued to proliferate during the succeeding 2 months. PBG cell proliferation was inversely correlated with the pancreatic islet loss. PBG cell hyperplasia was associated with the expansion and proliferation of Sox9/Ngn3-positive cells. Previously, Dipaola et al. indicated that proliferation of PBG cells occurs in experimental models of cholestasis [11]. Beside their role in the turnover of biliary epithelium, evidence has indicated that the biliary tree constitutes the stem cell reservoir also for endocrine pancreas [4]. In the developing pancreas, lineage-tracing experiments

demonstrated that all types of pancreatic epithelial cells have a common origin from Sox9-expressing progenitors [22, 23]. On the other hand, the role of Sox9-positive progenitor cells in maintaining the homeostasis of the adult pancreas has remained an important controversial issue [22, 24, 25].

Our recent findings indicated that BTSCs are precursors of committed progenitors within the pancreas [4]. In these studies, we showed that in vitro under the same conditions of serum-free KM, the hBTSCs were able to self-replicate indefinitely, whereas human fetal pancreatic cells were able initially to divide and undergo clonogenic expansion but after approximately eight divisions, the colonies transitioned into floating aggregates that underwent differentiation toward islet cells. The BTSCs remained as self-replicating cells but with the addition of various factors could be triggered at any time to go through a similar process to that of the pancreatic cells to form functional neoislets. Therefore, the pancreatic cells proved to be committed pancreatic progenitors, and the BTSCs could be lineage restricted to such progenitors by particular factors. Transplantation of these neoislets in vivo into diabetic mice resulted in an alleviation of hyperglycemia within 2 months [4].

In this study, we demonstrated that mouse PBGs activate as a consequence of pancreatic islet loss induced by STZ. Interestingly, previous reports indicated that pancreatic Sox9-positive ductal cells, ones present in pancreatic ductal glands, the known reservoirs of committed pancreatic progenitors, do not differentiate into endocrine cells in a STZ-induced diabetes model [26, 27]. In contrast, cells within PBGs rapidly and constantly proliferated, and the related Sox9/Ngn3-positive cell compartment was markedly expanded in our models. Moreover, STZ treatment was able to determine not only a proliferation but also a spatial reorganization of the PBG niches. In normal conditions, Sox9/Ngn3-positive cells were restricted to deeper PBG acini. After STZ treatments, Sox9/Ngn3-positive cells extended toward the surface epithelium.

Moreover, PBG cells at the hepatopancreatic ampulla showed the most prominent activation in terms of proliferation and insulin expression in comparison with those located at the hepatic hilum or cystic duct. A proximal-to-distal axis in the maturational lineages was described, going from stem cells in PBGs nearest to the duodenum to committed progenitors within the pancreatic duct glands in the pancreatic ducts [2, 11]. In addition, our data further support previous suggestions that PBGs at the level of the hepatopancreatic ampulla contain a reservoir of endodermal stem cells that include pancreatic stem cells and their descendants, pancreatic committed progenitors [4].

In parallel with Sox9 and Ngn3 expression, mouse PBG cells started to express insulin, thus indicating commitment toward a pancreatic endocrine lineage. RT-PCR showed a massive upregulation of insulin gene expression associated with the upregulation of *MafA* and *Gli1* genes. MafA is a key transcription factor for the terminal differentiation toward beta cells [28]. Gli-1 is crucial for pancreas development and in sustaining stem cell responses to regenerative needs [29].

To further translate our findings in humans, we evaluated the PBG compartment in T2D patients and the in vitro response of human BTSCs to high glucose concentration. In keeping with results obtained from the experimental models, PBGs at the hepatopancreatic ampulla from T2D subjects were hyperplastic, showed a higher proliferation rate, and contained more insulin positive cells. These in situ observations were paralleled by in vitro data. When hBTSCs were cultured under high glucose concentrations, they committed toward a pancreatic islet fate that included beta cells.

Taken together, our data indicate that high glucose concentrations are able to induce BTSC commitment toward pancreatic islet fates and that, in our models, BTSC activation induced by hyperglycemia is firstly characterized by BTSC proliferation and, subsequently, by the induction of beta cell differentiation.

In rodents, the presence of extrapancreatic insulin-producing cells has already been described in multiple organs and associated with experimental hyperglycemia [30]. In addition, cells exhibiting a glucose-stimulated insulin secretion have been described within EHBT [31, 32]. Moreover, studies in genetically manipulated animals have indicated that pancreatic differentiation could be induced in the biliary tract [33–35]. Finally, Sox9-positive cells in the liver and biliary tract can be reprogrammed to pancreatic cells by the overexpression of three transcription factors (*Pdx1, Ngn3*, and *MafA*), determining an improvement of glycemic profiles [8]. In this study, we show insulin-positive, duct-like structures ectopic to the pancreas and within the BTSC niches within the biliary tree represent a normal response to the administration of STZ, and their appearance is associated with the spontaneous upregulation of *MafA*.

Conclusion

Our data indicate that the PBG compartment is activated in diabetes, and the cells within the PBGs are involved in rescuing pancreatic islet loss. These data suggest that PBGs represent a target of genetic or pharmacological manipulations triggering their expansion and differentiation towards insulin-producing cells. In this light, our results open new approaches in the management of diabetes based on the modulation of the PBG niches.

Acknowledgments

We thank Raffaella Buzzetti (Department of Experimental Medicine, Sapienza University of Rome, Rome, Italy) for critical revision of the manuscript. E.G. was supported by research project grant from the University "Sapienza" of Rome, FIRB grant # RBAP10Z7FS_001, and by PRIN grant # 2009X84L84_001. D.A. was supported by FIRB grant # RBAP10Z7FS_004 and by PRIN grant # 2009X84L84_002. This study was also supported by Consorzio Interuniversitario Trapianti d'Organo, Rome, Italy, by a sponsored research agreement (SRAs) from Vesta Therapeutics (Bethesda, MD). L.M. Reid was funded by Vesta Therapeutics (Bethesda, MD), an NCI grant (CA182322) and the Lineberger Cancer Center grant (NCI grant # CA016086).

Author Contributions

G.C., R.P., and V.C.: conception and design, collection and assembly of data, data analyses and interpretation, manuscript writing, and final approval of manuscript; A.R.: collection and assembly of data, data analyses, manuscript writing, and final approval of manuscript; G.S.: data analyses and interpretation, manuscript editing, and final approval of

manuscript; L.N.: data analyses and interpretation, and final approval of manuscript; P.B.: collection and assembly of data, and final approval of manuscript; S.G.C. and M.R.: collection of materials and patients from type 2 diabetic patients and editing and final approval of the manuscript; L.R.: data analyses and interpretation, manuscript writing and editing, and final approval of manuscript; M.M., E.G., D.A.: financial support, conception and design, manuscript editing, and final approval of manuscript. G.C., R.P. and V.C. contributed equally to this work. M.M., E.G., and D.A. are co-equal senior authors.

Disclosure of Potential Conflicts of Interest

The authors indicate no potential conflicts of interest. An exception is that L.M.R. has an equity position in a company, PhoenixSongs Biologicals, that has a license for nonclinical uses of some of the IP generated in her lab.

References

1 Cardinale V, Wang Y, Carpino G et al. The biliary tree—A reservoir of multipotent stem cells. Nat Rev Gastroenterol Hepatol 2012;9:231-240.

2 Carpino G, Cardinale V, Onori P et al. Biliary tree stem/progenitor cells in glands of extrahepatic and intraheptic bile ducts: An anatomical in situ study yielding evidence of maturational lineages. J Anat 2012;220:186-199.

3 Cardinale V, Wang Y, Carpino G et al. Multipotent stem/progenitor cells in human biliary tree give rise to hepatocytes, cholangiocytes, and pancreatic islets. Hepatology 2011;54:2159-2172.

4 Wang Y, Lanzoni G, Carpino G et al. Biliary tree stem cells, precursors to pancreatic committed progenitors: Evidence for possible life-long pancreatic organogenesis. Stem Cells 2013;31:1966-1979.

5 Carpino G, Cardinale V, Gentile R et al. Evidence for multipotent endodermal stem/progenitor cell populations in human gallbladder. J Hepatol 2014;60:1194-1202.

6 Spence JR, Lange AW, Lin SC et al. Sox17 regulates organ lineage segregation of ventral foregut progenitor cells. Dev Cell 2009;17:62-74.

7 Zaret KS. Genetic programming of liver and pancreas progenitors: Lessons for stem-cell differentiation. Nat Rev Genet 2008;9:329-340.

8 Banga A, Akinci E, Greder LV et al. In vivo reprogramming of Sox9 + cells in the liver to insulin-secreting ducts. Proc Natl Acad Sci USA 2012;109:15336-15341.

9 Grieco FA, Moretti M, Sebastiani G et al. Delta-cell-specific expression of hedgehog pathway Ptch1 receptor in murine and human endocrine pancreas. Diabetes 2011;27:755-760.

10 Leiter EH, Schile A. Genetic and pharmacologic models for Type 1 diabetes. Curr Protoc Mouse Biol 2013;3:9-19.

11 Dipaola F, Shivakumar P, Pfister J et al. Identification of intramural epithelial networks linked to peribiliary glands that express progenitor cell markers and proliferate after injury in mice. Hepatology 2013;58:1486-1496.

12 Nobili V, Carpino G, Alisi A et al. Role of docosahexaenoic acid treatment in improving liver histology in pediatric nonalcoholic fatty liver disease. PLoS One 2014;9:e88005.

13 Mancinelli R, Onori P, Gaudio E et al. Taurocholate feeding to bile duct ligated rats prevents caffeic acid-induced bile duct damage by changes in cholangiocyte VEGF expression. Exp Biol Med 2009;234:462-474.

14 Yang F, Priester S, Onori P et al. Castration inhibits biliary proliferation induced by bile duct obstruction: Novel role for the autocrine trophic effect of testosterone. Am J Physiol Gastrointest Liver Physiol 2011;301:G981-G991.

15 Onori P, Wise C, Gaudio E et al. Secretin inhibits cholangiocarcinoma growth via dysregulation of the cAMP-dependent signaling mechanisms of secretin receptor. Int J Cancer 2010;127:43-54.

16 Chomczynski P, Sacchi N. The single-step method of RNA isolation by acid guanidinium thiocyanate-phenol-chloroform extraction: Twenty-something years on. Nat Protoc 2006;1:581-585.

17 Cantafora A, Blotta I, Rivabene R et al. Evaluation of RNA messengers involved in lipid trafficking of human intestinal cells by reverse-transcription polymerase chain reaction with competimer technology and microchip electrophoresis. Electrophoresis 2003;24:3748-3754.

18 Cardinale V, Wang Y, Carpino G et al. Multipotent stem cells in the biliary tree. Ital J Anat Embryol 2010;115:85-90.

19 Lanzoni G, Oikawa T, Wang Y et al. Concise review: Clinical programs of stem cell therapies for liver and pancreas. Stem Cells 2013;31:2047-2060.

20 Semeraro R, Carpino G, Cardinale V et al. Multipotent stem/progenitor cells in the human foetal biliary tree. J Hepatol 2012;57:987-994.

21 Lanzoni G, Cardinale V, Carpino G. The hepatic, biliary and pancreatic network of stem/progenitor cells niches in humans: A new reference frame for disease and regeneration. Hepatology 2015 [Epub ahead of print].

22 Kawaguchi Y. Sox9 and programming of liver and pancreatic progenitors. J Clin Invest 2013;123:1881-1886.

23 Seymour PA, Freude KK, Dubois CL et al. A dosage-dependent requirement for Sox9 in pancreatic endocrine cell formation. Dev Biol 2008;323:19-30.

24 Hosokawa S, Furuyama K, Horiguchi M et al. Impact of Sox9 dosage and Hes1-mediated Notch signaling in controlling the plasticity of adult pancreatic duct cells in mice. Sci Rep 2015;5:8518.

25 Huch M, Bonfanti P, Boj SF et al. Unlimited in vitro expansion of adult bi-potent pancreas progenitors through the Lgr5/R-spondin axis. EMBO J 2013;32:2708-2721.

26 Furuyama K, Kawaguchi Y, Akiyama H et al. Continuous cell supply from a Sox9-expressing progenitor zone in adult liver, exocrine pancreas and intestine. Nat Genet 2011;43:34-41.

27 Kopp JL, Dubois CL, Hao E et al. Progenitor cell domains in the developing and adult pancreas. Cell Cycle 2011;10:1921-1927.

28 Lysy PA, Weir GC, Bonner-Weir S. Concise review: Pancreas regeneration: Recent advances and perspectives. Stem Cells Transl Med 2012;1:150-159.

29 Hsu YC, Li L, Fuchs E. Transit-amplifying cells orchestrate stem cell activity and tissue regeneration. Cell 2014;157:935-949.

30 Kojima H, Fujimiya M, Matsumura K et al. Extrapancreatic insulin-producing cells in multiple organs in diabetes. Proc Natl Acad Sci USA 2004;101:2458-2463.

31 Dutton JR, Chillingworth NL, Eberhard D et al. Beta cells occur naturally in extrahepatic bile ducts of mice. J Cell Sci 2007;120:239-245.

32 Nagaya M, Katsuta H, Kaneto H et al. Adult mouse intrahepatic biliary epithelial cells induced in vitro to become insulin-producing cells. J Endocrinol 2009;201:37-47.

33 Eberhard D, Tosh D, Slack JM. Origin of pancreatic endocrine cells from biliary duct epithelium. Cell Mol Life Sci 2008;65:3467-3480.

34 Fukuda A, Kawaguchi Y, Furuyama K et al. Ectopic pancreas formation in Hes1-knockout mice reveals plasticity of endodermal progenitors of the gut, bile duct, and pancreas. J Clin Invest 2006;116:1484-1493.

35 Sumazaki R, Shiojiri N, Isoyama S et al. Conversion of biliary system to pancreatic tissue in Hes1-deficient mice. Nat Genet 2004;36:83-87.

See www.StemCells.com for supporting information available online.